Available online at www.sciencedirect.com
ScienceDirect
Journal of Magnetic Resonance 190 (2008) 183–188
JMR Journal of Magnetic Resonance
www.elsevier.com/locate/jmr

Optimum pulse flip angles for multi-scan acquisition of hyperpolarized NMR and MRI

Kaz Nagashima

Tokyo Magnetic Resonance, Inc., 31 Daikyo-cho, Shinjuku City, Tokyo 160-0015, Japan

Received 15 April 2007; revised 30 September 2007
Available online 30 October 2007

Abstract

The optimum pulse flip angles were calculated for multi-scan acquisition of hyperpolarized NMR and MRI. The derived formulae could be correlated with the best angle for ordinary steady-state acquisition, the so-called Ernst angle. Although single-scan acquisition has been popular in hyperpolarized measurements, signal accumulation by increasing scans may become very effective for improving the total signal gain, especially when the sample's longitudinal spin relaxation time is long. The optimum angles were calculated from theoretical relations between the exponential of the pulse repetition time/relaxation time ratio and the total scan counts. Constant and variable flip angle cases are presented, both of which yield similar cumulative signal amplitudes. For the constant angle case, a numerically calculated semi-universal curve is presented for the rough estimation of the best angle, as the results were not significantly dependent upon the degree of hyperpolarization within the realistic range. Meanwhile, for the variable angle case, the best angles were approximated from a clean trigonometric series relation, in which the initial pulse became near the Ernst angle and the last pulse was always 90°. A modification of the variable angle scheme enables the acquisition of uniform signal amplitude throughout all scans.

Keywords: Hyperpolarization; Ernst angle; Variable flip angle

1. Introduction

Hyperpolarization, such as dynamic nuclear polarization [1] and optical pumping [2,3], realizes enormous signal enhancement in magnetic resonance. It has even made possible obtaining ^{13}C NMR in low-concentration samples [4] and dynamic diagnostic MRI of lung using noble gases [5]. With the recent availability of commercial hyperpolarizers, such as HyperSense™ (Oxford Instruments, UK), Xe-BoxB™ (Xemed, NH), and HPXE2100™ (Toyoko Kagaku, Japan), this state-of-the-art technique is expected to become routine for walk-up spectrometer runs by students and in regular health checkups.

In hyperpolarized NMR measurements, the nuclear magnetization of the sample is pre-enhanced outside the main magnet to, say, more than 1% excess of spin population, and the preparation may become cumbersome and lengthy if a high degree of polarization is pursued. The highly polarized sample is then swiftly transferred into the NMR probe for observation before spin relaxation takes place. Often, only one 90° pulse is applied in the acquisition step in order to fully and quickly utilize the strong magnetization. However, this single-shot method poses a problem if satisfactory polarization has not been achieved or the spectrometer's software or hardware is incorrectly set; in the worst-case scenario, the entire processes must be repeated from the beginning.

A simple solution for such issues may be just to increase the number of scans, as signal summation will increase the total signal amplitude and provide a better possibility of acquiring useable data. This report presents the best flip angles for the multi-scan acquisition of hyperpolarized samples. Zhao et al. [6] have previously reported some key equations for variable flip angle measurements of hyperpolarized gas MRI, in which uniform signal ampli-

E-mail address: kaznaga@gmail.com

1090-7807/$ - see front matter © 2007 Elsevier Inc. All rights reserved.
doi:10.1016/j.jmr.2007.10.011

tude was sought throughout whole scans. The draft of this report was prepared and submitted with no knowledge of their studies, and some overlaps were actually found in the revision step. The novel features of the present study are that the maximization of the cumulative signal amplitude is attempted with signal summation, both the constant and variable flip angle schemes are considered, and the theoretical setups are simple. Although the presented contents would not be directly applicable to parahydrogen-induced polarization (PHIP) [7], the modification might lead to better usage of the enhanced magnetization even in this case.

2. Theory

Utilization of the Ernst angle [8] is an effective method for shortening measurement times of otherwise time-consuming experiments, e.g., 1D ^{13}C NMR of coals [9], 2D NMR of proteins [10,11], and 3D MRI of the human body [12,13]. Its concise equation shows up in virtually all contemporary NMR textbooks:

$$\beta_{Ernst} = \cos^{-1} E_1, \tag{1}$$

where $E_1 = \exp(-\mathrm{TR}/T_1)$, in which TR is repetition duration between pulses and T_1 is longitudinal relaxation time of sample nuclei. The derivation assumes on-resonance acquisition in the steady state after applying several dummy pulses. In measurements of hyperpolarized samples, dummy pulses are usually not used because the pre-enhanced magnetization must be used as quickly as possible. Such a dynamic state, where the polarization decays from hyperpolarized state (initial state) to near thermal equilibrium might be referred to as a depolarization state. The decay behavior and the physical states of magnetization are schematically illustrated in Fig. 1. Their details for the constant and variable flip angle cases will be discussed separately below.

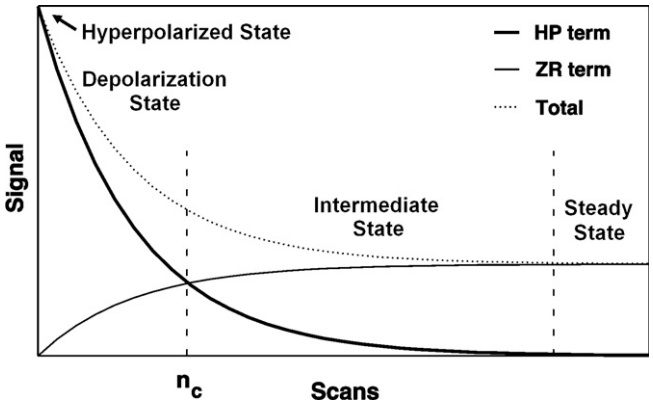

Fig. 1. Schematic representation of the contributions of the HP term, the ZR term, and their sum to the signal decay of a hyperpolarized sample. In this figure, the magnitude of the ZR term is overly exaggerated for clarity; it would be much smaller than the HP term in actual hyperpolarized experiments. The regions of the magnetization decay curve may be categorized into the four states, as indicated. The critical number of scans (n_c) is defined at the crossing point of the HP and ZR terms.

In this report, the terms "equilibrium magnetization" and "steady-state magnetization" have distinct meanings. The former is tantamount to what NMR/MRI people call M_0, which is attained with elapse of an infinitely long time after a sample is set into a static magnetic field. The latter is attained after applying several pulses to the former, although its onset is difficult to define. For simplicity, the signal decays due to transverse magnetization and diffusion will not be taken into account, even though they may become non-negligible factors, for example, when a flip-back type imaging [14] is exercised. Also, this report concentrates on the maximization of the cumulative signal and not of the signal-to-noise (S/N) ratio; the latter naively depends on how baseline, noise, and signal heights are defined, which would require rigorous statistical treatments.

2.1. Constant flip angle scheme

A minor modification on the Ernst angle's derivation procedure [8] leads to a magnetization equation for the depolarization state after n pulses. The x component of magnetization observed immediately after the nth pulse is given by

$$M_{x,n} = \pm M_{\mathrm{hp}}(E_1 \cos\beta)^{n-1} \sin\beta + M_0(1-E_1)\sum_{k=1}^{n-1}(E_1\cos\beta)^{k-1}\sin\beta, \tag{2}$$

where M_{hp} is the initial magnetization at the hyperpolarized state, M_0 is the magnetization in thermal equilibrium, and β is the flip angle of the pulse. The $\pm$sign changes depending upon the direction of pre-polarization with respect to the static magnetic field and also upon the sign of the gyromagnetic ratio of the nuclei. For simplicity, only the positive case is considered.

The balance of the first and second terms of Eq. (2) is relevant when trying to analyze the signal decay. The terms are short-handedly expressed as the HP term and the ZR term, respectively. Intuitively, the ZR term becomes negligibly small compared to the HP term if a highly pre-polarized sample is observed in low field (viz., $M_{\mathrm{hp}}/M_0 \sim \infty$) or the sample's T_1 is much longer than TR (i.e., $E_1 \sim 1$). In order to more analytically interpret the equation, the HP term is converted to a decreasing exponential as a function of n:

$$\mathrm{HP} = M_{\mathrm{hp}} \sin\beta \exp\left[-\ln\left(\frac{1}{E_1\cos\beta}\right)(n-1)\right]. \tag{3}$$

This component originates purely from a hyperpolarized magnetization. On the other hand, using a geometric series relation, the ZR term can be rewritten as

$$\mathrm{ZR} = M_0(1-E_1)\sin\beta\frac{1-(E_1\cos\beta)^{n-1}}{1-E_1\cos\beta}, \tag{4}$$

which increases asymptotically to a constant value, $M_0(1-E_1)\sin\beta/(1-E_1\cos\beta)$, as n increases. This component is attributable to the spin-relaxed magnetization, i.e., regular magnetization build-up. A critical number of scans (n_c) can then be defined at the crossing point of the HP and ZR terms:

$$n_c = 1 + \frac{\ln\left[\frac{(1-E_1)}{(M_{hp}/M_0)(1-E_1\cos\beta)+(1-E_1)}\right]}{\ln(E_1\cos\beta)}. \quad (5)$$

For a limiting case of $\beta = 0$ ($\cos\beta = 1$), Eq. (5) can be simplified to $n_c = 1 - \ln[(M_{hp}/M_0)+1]/\ln E_1$ and the total z-magnetization becomes $\sim 2M_0$ if the degree of polarization is high. n_c may be regarded as a scale for the duration of the depolarization state, before the end of which one may want to finish data acquisition.

As the summation of Eq. (2) does not appear to simplify to a terse mathematical expression, the best flip angle for maximum cumulative signal would have to be numerically calculated. But, the following formula might be useful for quick spreadsheet calculation:

$$\frac{1-x^{n_{max}}}{1-n_{max}x^{n_{max}-1}+(n_{max}-1)x^{n_{max}}} = \frac{E_1^2-x^2}{x(1-x)}, \quad (6)$$

where n_{max} is the total number of scans to be acquired and $x = E_1\cos\beta$. The equation can be derived by zeroing β-derivative of the sum of the HP term, $\frac{d}{d\beta}\sin\beta\sum_{k=1}^{n}(E_1\cos\beta)^{k-1}$, ignoring the contribution of the ZR term. The optimum flip angle gets closer to the Ernst angle when n_{max} is large, since the left-hand side of Eq. (6) approaches 1.

2.2. Variable flip angle scheme

When the pulse flip angle is changed at each scan, Eq. (2) can be modified to

$$M_{x,n} = M_{hp}\left[\prod_{k=1}^{n-1}(E_1\cos\beta_k) + \frac{1}{M_{hp}/M_0}(1-E_1)\times\left\{\sum_{i=2}^{n}\prod_{k=i}^{n-1}(E_1\cos\beta_k)\right\}\right]\sin\beta_n, \quad (7)$$

where β_n is the flip angle at the nth pulse. The first term is found to be equivalent to the equation derived by Zhao et al. [6]. If a high degree of pre-polarization is achieved ($M_{hp}/M_0 \sim \infty$) or the relaxation time is long ($E_1 \sim 1$), the second term becomes negligible. In such a case, the optimum flip angles can be calculated by first differentiating the cumulative sum $\left(S = \sum_{i=1}^{n}\prod_{k=1}^{i-1}(E_1\cos\beta_k)\right)$ by all β_n's. Then, by simultaneously zeroing all of the n differential equations, i.e., $dS/d\beta_1 = dS/d\beta_2 = \cdots dS/d\beta_n = 0$, a clean series relation can be reached:

$$\beta_n = \cos^{-1}\sqrt{\frac{E_1^2 - E_1^{2(n_{max}-n+1)}}{1-E_1^{2(n_{max}-n+1)}}}. \quad (8)$$

At the beginning of the scans, i.e., for small n, β_n takes a value close to β_{Ernst}, particularly when n_{max} is large. In a variable flip angle scheme, when the cumulative signal intensity is to be maximized, the flip angle for the last pulse always becomes 90°, regardless of E_1. Earlier pulse angles may be iteratively back-calculated from the last pulse by $\tan\beta_n = \sin\beta_{n+1}/E_1$, from which Eq. (8) was obtained.

In FLASH-type imaging or reaction rate measurement on hyperpolarized samples, one may want to have the same signal amplitude at each excitation. Setting β_n^{flat} as the pulse angle for the special case, the relation $\tan\beta_n^{flat} = E_1\sin\beta_{n+1}^{flat}$ can be obtained, which leads to the following general solution:

$$\beta_n^{flat} = \cos^{-1}\sqrt{\frac{1-E_1^{(2n_{max}-2n-1)}}{1-E_1^{2(n_{max}-n+1)}}}. \quad (9)$$

In this case as well, a 90° pulse is applied at the last scan to maximize the signal intensity. Earlier pulse angles are then adjusted in such a way that a constant signal amplitude is obtained throughout all scans.

3. Results and discussion

The degree of hyperpolarization (P), NMR frequency in static magnetic field (f_0), and the temperature (T) determine the magnitude of M_{hp}/M_0 ($= 2PkT/f_0h$ for spin 1/2 nuclei, in which k and h are Boltzmann and Planck constants). For example, when 1% hyperpolarized ^{129}Xe is observed at 9.4 T at room temperature, $M_{hp}/M_0 \sim 1100$. In this report, the signal acquisition was assumed to be on-resonance, M_{hp}/M_0 was set to 1000 as a default value, and the intensities were normalized by $M_{hp}(=1)$, unless otherwise stated. Also, notice that the figures below contain "signal amplitude" observed in each scan and "cumulative signal amplitude," which results in after signal summations.

3.1. Constant flip angle scheme

Simulated signal decays are displayed in Fig. 2 as a function of scan count. In Fig. 2a, the calculated signal decays for three different pulse angles, 30°, 60°, and 90°, are compared at $TR/T_1 = 0.1$. The signal decays with 30° and 60° pulses are almost purely exponential because the maximum scan count is 8, which is much less than the n_c values for the two angles, 12 and 33 scans, respectively. In contrast, one 90° pulse ($n_c = 1$) leaves essentially no magnetization along the z-direction for the subsequent scans and, obviously, the steep fall down is not exponential. Shown in Fig. 2b is the TR/T_1 dependency of signal decay, in which the flip angle was fixed at 30°. As expected, one single pulse yields the same signal amplitude for all TR/T_1 values. When $TR/T_1 = 0.01$ and 0.1, the signal intensity at each scan decays exponentially ($R^2 > 0.9999$). The $TR/T_1 = 1$ data ($n_c \sim 7$) are, by contrast, non-exponential, albeit a low-angle pulse is used. Evidently, care must be taken whenever the signal decay of a hyperpolarized sample is exponentially fitted for

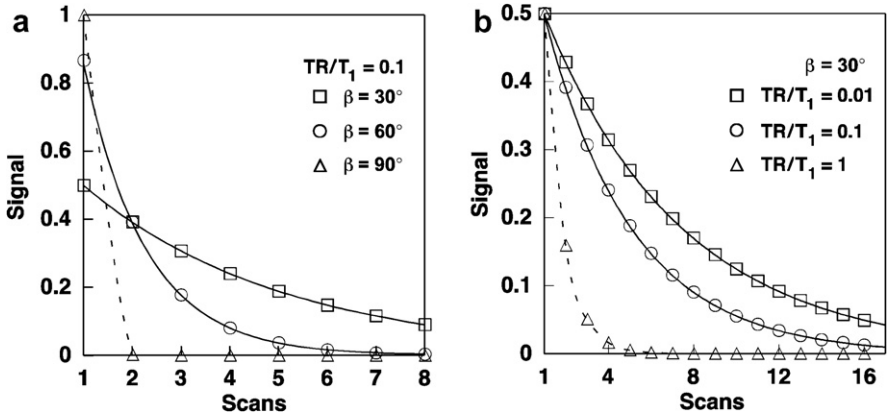

Fig. 2. Simulated signal intensity of a hyperpolarized sample as a function of scan count ($M_{hp}/M_0 = 1000$ and $M_{hp} = 1$). (a) At $TR/T_1 = 0.1$, the pulse angle was set to 30°, 60°, and 90°, respectively. For 30° and 60°, the calculated signal decays are nearly perfectly exponential, as indicated by the solid lines. A 90° pulse at the first scan leaves essentially no magnetization for later scans, and the decay cannot be exponentially fitted; the dashed line is a spline interpolation just to guide the eye. (b) The pulse angle was fixed to 30° and then TR/T_1 was set to 0.01, 0.1, and 1, respectively. As expected, the signal intensities for the first pulse become the same for all cases. For $TR/T_1 = 0.01$ and 0.1, the signal reduction is nearly perfectly exponential, as fitted with solid lines. But in the case of $TR/T_1 = 1$, the intensity loss could no longer be approximated with an exponential function, so a spline interpolation, as displayed with the dashed line, was used to guide the eye.

some data analysis, even if a relatively low pulse angle is used.

Fig. 3 shows the cumulative signal amplitude calculated from the sum of Eq. (2) for three different TR/T_1s. The best flip angle shifts from 90° to the low-angle side and gets closer to the Ernst angle as the number of scans increases. Multi-scan experiments may be particularly effective for signal enhancement, provided the sample's T_1 is long and TR can be set to a small value. For example, when 16 scans are acquired at $TR/T_1 = 0.01$ and 0.1, more than a two- to threefold higher signal gain can be expected than with a single-shot measurement by 90° pulse. However, for $TR/T_1 = 1$, signal summations after four scans would just degrade the data quality, as the overlapping curves imply. Realistically, the maximum number for multi-scan acquisition of a hyperpolarized sample should be set less than n_c.

Plotted in Fig. 4 are the optimum flip angles numerically calculated from Eq. (2). The calculated curves were almost independent of M_{hp}/M_0 within its realistic range, so the figure may be used for a rough estimation of β^{opt}. Before the spectrometer run, one must plan the total number of scans and the best flip angle for it with *a priori* known T_1 information. If an expected TR/T_1 value cannot be less than 0.1, use of the Ernst angle would be a reasonable choice. In any case, TR should be minimized whenever signal summation is intended. This makes a stark contrast to ordinary NMR experiments in near-thermal equilibrium, where TR of $1T_1$ to $5T_1$ is typically used for magnetization recovery.

3.2. Variable flip angle scheme

The optimum angle in a variable flip angle scheme, calculated from Eq. (8), is depicted in Fig. 5. The flip angle is

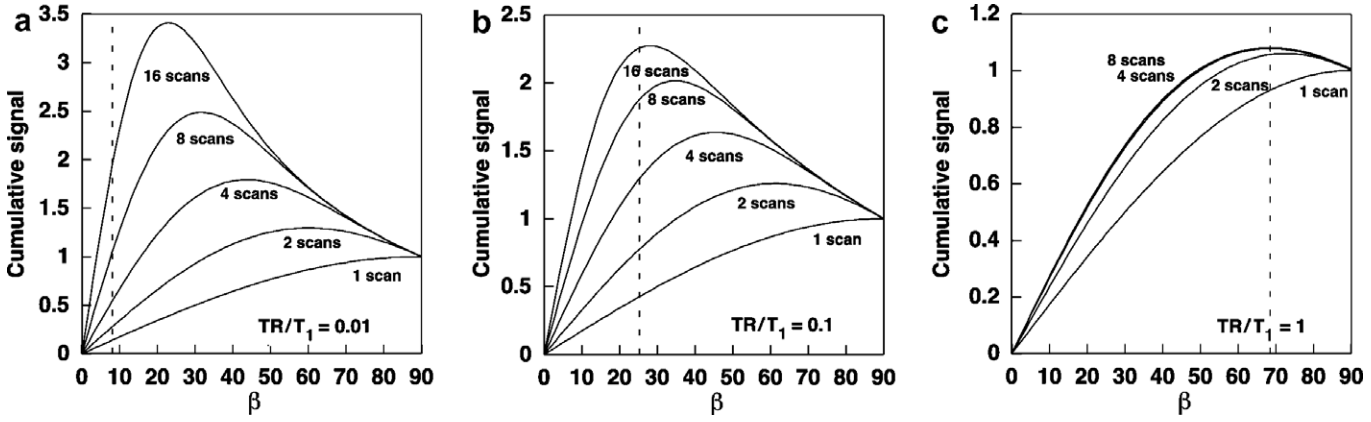

Fig. 3. Cumulative signal intensities as a function of pulse flip angle ($M_{hp}/M_0 = 1000$). Based on Eq. (2), the signal intensities from first to sixteenth scans were summed in order to evaluate the overall intensity. Dashed lines indicate the Ernst angles at each TR/T_1, to which the optimum pulse angle, i.e., the peak of the curve, accesses as scan counts increase. When TR/T_1 is less than 0.1, increasing scan counts may become very effective for signal enhancement. In this particular example, 16 times of signal summations lead to a roughly two- to threefold higher signal than a single scan with one 90° pulse. In contrast, for $TR/T_1 = 1$, signal summations after four scans are of no additional value, as is evident from the overlapping four- and eight-scan curves.

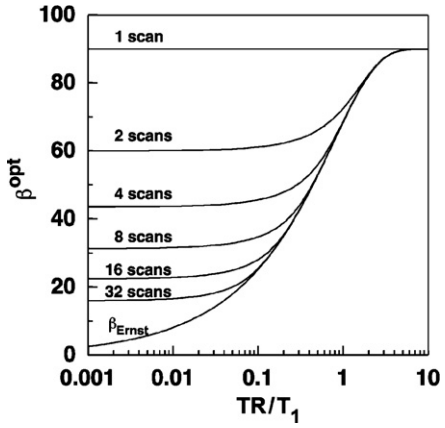

Fig. 4. Optimum pulse angles for the measurement of a hyperpolarized sample as a function of TR/T_1. The results were numerically calculated from the sum of Eq. (2). Indicated over the curves are the total numbers of scans to be acquired. Although these data were calculated at $M_{hp}/M_0 = 1000$, results were not very sensitive to M_{hp}/M_0 within the realistic range ($M_{hp}/M_0 = 10^1 \sim 10^5$). Therefore, this figure may be used for a rough estimation in actual measurements. When a large total scan number is chosen for the measurement, the best angle gets closer to the Ernst angle. When TR/T_1 is more than 2, the best flip angle for multi-pulse acquisition is always equal to the Ernst angle.

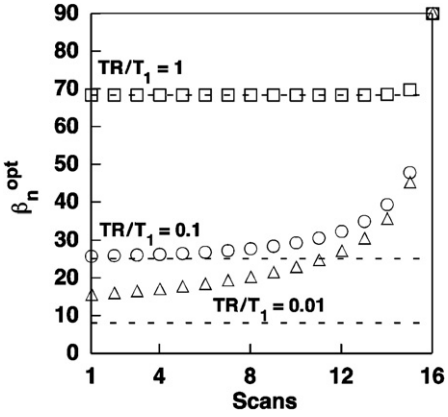

Fig. 5. Optimum pulse angles as a function of scan count in variable flip angle measurement. The results were calculated from Eq. (8), assuming $n_{max} = 16$. The best angle for the last pulse always becomes 90° in the variable flip angle scheme, regardless of TR/T_1. Dashed lines indicate Ernst angles for each TR/T_1; the angle for the initial pulses gets closer to the Ernst angle when TR/T_1 is large.

altered at each scan in this case. In order to maximize the cumulative signal amplitude, the last pulse angle should be set to 90°, regardless of TR/T_1. At $n_{max} = 16$ and $TR/T_1 = 1$, the best angle for the initial scans is near the Ernst angle, and it does not significantly increase until the last pulse. However, this is not the case for low TR/T_1, which displays a gradual increase in flip angle from an initial value slightly larger than the Ernst angle.

The cumulative signal amplitude as a function of n_{max} is shown in Fig. 6, in which the results of constant and variable flip angle schemes are compared. The cumulative signal by the variable flip angle scheme may become higher than by the constant flip angle scheme when n_{max} is small.

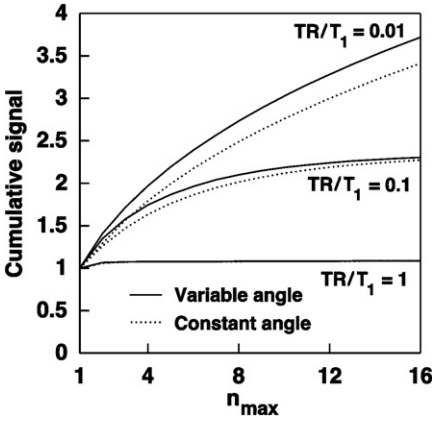

Fig. 6. Cumulative signal intensity of a hyperpolarized sample as a function of the total number of scans ($M_{hp}/M_0 = 1000$). Variable (solid line) and constant flip angle (dashed line) schemes with three different TR/T_1 values are compared. When $TR/T_1 = 1$, the signal increase after the first pulse is not significant, even if scans are continued. In low-TR/T_1 cases, the variable flip angle scheme may result in higher cumulative signals, particularly when the total number of scans is relatively low, say less than 16. If TR can be set to a small value, the signal gain may be significantly improved by scan repetitions.

But the difference is trivial when TR/T_1 is more than 0.1, and they will yield almost the same total signal amplitude as the number of scans increases. With 16 scans of signal summation, the amplitude is 1.1 for $TR/T_1 = 1$ and 2.3 for $TR/T_1 = 0.1$, and both of the case reached their plateau values. But for the $TR/T_1 = 0.01$ case, the efficacy of signal summation continues even after 16 scans, at which 3.7-fold-higher intensity has already been attained.

Theoretically, the variable flip angle scheme can be modified for observing constant signal amplitude at each pulse. By sacrificing a couple of initial scans for receiver gain adjustment, this method could allow a better use of the

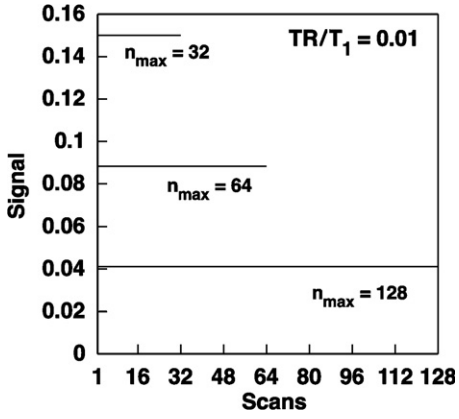

Fig. 7. Simulated signal intensity of a hyperpolarized sample with flat-amplitude variable flip angle method ($TR/T_1 = 0.01$, $M_{hp}/M_0 = 1000$). The last pulse's flip angle was set to 90° in order to maximize signal intensity and the earlier pulse angles were back-calculated by the relation $\tan\beta_n^{flat} = E_1 \sin\beta_{n+1}^{flat}$. The signal intensity after each pulse was calculated from Eq. (7). Although the expected signal amplitude decreases to about 4% to 15% of single pulse acquisition ($M_{hp} = 1$), it is still more than 40-fold-higher than the steady-state acquisition ($M_x^{steady\ state} < M_0 = 0.001$).

spectrometer's dynamic range. Possible applications are imaging [6], angiography, and reaction rate measurements, although the estimation of the sample's T_1 is a prerequisite for the method's adaptation. The resulting signal amplitude calculated from Eq. (7) with the β_n^{flat} values is shown in Fig. 7. If the signal amplitude is forced to be uniform throughout all scans, some signal intensity has to be sacrificed. Unavoidably, the total number of scans must be decreased whenever high signal amplitude is sought. However, although the degree of polarization was assumed to be relatively small ($M_{\text{hp}}/M_0 = 1000$), the calculated results still have more than 4% of the intensity of a single 90° pulse ($1 = M_{\text{hp}}$). Even the $n_{\max} = 128$ case leads to more than a 40-fold-stronger signal than steady-state acquisition ($M_x^{\text{steady state}} < M_0 = 0.001$). In any case, it must be remembered that, if spin relaxation is too fast, hyperpolarized techniques are not very effective for improving the data quality of NMR and MRI.

4. Conclusions

Although single-shot acquisition has been popular in hyperpolarized NMR measurements, increasing scan counts may be effective for enhancing total signal amplitude, especially when the sample's relaxation time (T_1) is long. Choice of constant or variable flip angle scheme should be determined individually for each case. The time for pulse repetition (TR) must be minimized in the depolarization state measurements by implementing a short acquisition time (viz., the number of data points multiplied by the dwell time) and removing relaxation (recycle) delay. By modifying the variable angle method, a uniform flat signal amplitude can be obtained in a series of pulse excitations, in which receiver gain adjustment would be possible.

Lastly, it should be stated that the contents of this report are still nascent and a plethora of problems remain to be solved for realizing the ultimate goal, i.e., more widespread uses of hyperpolarized NMR and MRI. Topics left for future studies are experimental verification of the results in this report, the derivation of a succinct β^{opt} equation for the constant angle scheme, n_c equation for the variable angle scheme, numerical solving of optimum angles for the variable angle scheme, the optimum angles in cumulative acquisition of PHIP, and the S/N ratio relations of these.

References

[1] J.H. Ardenkjær-Larsen, B. Fridlund, A. Gram, G. Hansson, L. Hansson, M.H. Lerche, R. Servin, M. Thaning, K. Golman, Increase in signal-to-noise ratio of >10,000 times in liquid-state NMR, Proc. Natl. Acad. Sci. USA. 100 (2003) 10158–10163.

[2] M.S. Albert, G.D. Cates, B. Driehuys, W. Happer, B. Saam, C.S. Springer, A. Wishinia, Biological magnetic resonance imaging using laser-polarized ^{129}Xe, Nature 370 (1994) 199–201.

[3] G. Navon, Y.-Q. Song, S. Appelt, R.E. Taylor, A. Pines, Enhancement of solution NMR and MRI with laser-polarized xenon, Science 271 (1996) 1848–1851.

[4] C.-G. Joo, K.-N. Hu, J.A. Bryant, R.G. Griffin, In situ temperature jump high-frequency dynamic nuclear polarization experiments: enhanced sensitivity in liquid-state NMR spectroscopy, J. Am. Chem. Soc. 128 (2006) 9428–9432.

[5] S. Månsson, A.J. Deninger, P. Magnusson, G. Pettersson, L.E. Olsson, G. Hansson, P. Wollmer, K. Golman, ^{3}He MRI-based assessment of posture-dependent regional ventilation gradients in rats, J. Appl. Physiol. 98 (2005) 2259–2267.

[6] L. Zhao, R. Mulkern, C.-H. Tseng, D.L. Williamson, S. Patz, R. Kraft, R.L. Walsworth, F.A. Jolesz, M.S. Albert, Gradient-echo imaging considerations for hyperpolarized ^{129}Xe MR, J. Magn. Reson. B 113 (1996) 179–183.

[7] J. Natterer, J. Bargon, Parahydrogen induced polarization, Prog. NMR Spectrosc. 31 (1997) 293–315.

[8] R.R. Ernst, G. Bodenhausen, A. Wokaun, Principles of Nuclear Magnetic Resonance in One and Two Dimensions, Clarendon Press, Oxford, 1987.

[9] R.E. Botto, Optimization of sensitivity in pulsed ^{13}C NMR of coals, Energy Fuels 16 (2002) 925–927.

[10] P. Schanda, B. Brutscher, SOFAST-HMQC experiments for recording two-dimensional heteronuclear correlation spectra of proteins within a few seconds, J. Biomol. NMR 33 (2005) 199–211.

[11] A. Ross, M. Saltzmann, H. Senn, Fast-HMQC using Ernst angle pulses: an efficient tool for screening of ligand binding to target proteins, J. Biomol. NMR 10 (1997) 389–396.

[12] G. Steidle, H. Graf, F. Schick, Sodium 3-D MRI of the human torso using a volume coil, Magn. Reson. Imaging 22 (2004) 171–180.

[13] G. Johnson, Y.Z. Wadghiri, D.H. Turnbull, 2D multislice and 3D MRI sequences are often equally sensitive, Magn. Reson. Med. 41 (1999) 824–828.

[14] J. Svensson, S. Mänsson, E. Johansson, J.S. Petersson, L.E. Olesson, Hyperpolarized ^{13}C MR angiography using TrueFISP, Magn. Reson. Med. 50 (2003) 256–262.